A FORCE MODEL FOR SUPERFINISH TURNING OF PURE COPPER WITH ROUNDED EDGE TOOLS AT LOW FEED RATE

D. GERMAIN[1, 2, *], G. FROMENTIN[2], G. POULACHON[2], and S. BISSEY–BRETON[1]

[1]*CEA, DAM, Valduc, 21120 Is-sur-Tille, France*
[2]*Arts et Metiers ParisTech, LaBoMaP, rue Porte de Paris, 71250 Cluny, France*

Abstract: This paper presents a model for force prediction of superfinish turning operation on pure copper. The model is divided in two parts. The first part computes the forces acting on the rake face of the tool. The second part computes the forces on the clearance face that are much more important in superfinish machining than in conventional machining.

Keywords: Cutting forces, edge geometry, superfinish turning, pure copper, scale effect

1 INTRODUCTION

The modelling of cutting forces has been widely explored among the last decades in order to achieve optimum quality in machining, improve cutting tools and machine-tool capability. It is also still a helpful data for workpiece deformation or surface integrity predictive models. When preliminary tests cannot be performed before production starts, a physically significant model may provide enough information for the qualification of the tool geometry or even the machine-tool without producing any chip. Superfinish machining involves low feed rates, thus, uncut chip thickness is thin in front of the edge radius. Several strategies, like the mechanistic models based on the model of (Kienzle 52), exists to predict the forces but often requires a large batch of experimental data to calibrate their constants. This paper presents an analytical model for the prediction of forces in cutting of pure copper considering the scale effects encountered in superfinishing operations in the case of orthogonal machining.

2 DEVELOPED APPROACH

This work is based on an analytical and mechanical study of a continuous chip formation process. Let us consider the simple case of orthogonal machining. In this case, the forces are all in the same plane containing feed and cutting velocity. The work material is a pure copper with elasto-plastic mechanical behaviour. As shown on figure 1 the tool has a rounded edge and a positive rake angle.

2.1 Forces on the rake face

The primary shear zone is assumed without any curvature and in plane strain state with a constant shear strength along the shear plane (Thomsen 65). Two resultant forces are assumed; one acting on the rake face (R) due to the action of the chip on the tool and one on the clearance face (C) due to the contact with the machined surface. Those resultants are then decomposed along the cutting direction (c) and the thrust direction (t), and expressed in equation (1). The forces $F_{c,R}$ and $F_{t,R}$ acting on the rake face are the result of the plastic deformation of the work material in the primary shear zone oriented by the shear angle ϕ.

$$F_c = F_{c,R} + F_{c,C}, \qquad F_t = F_{t,R} + F_{t,C}. \tag{1}$$

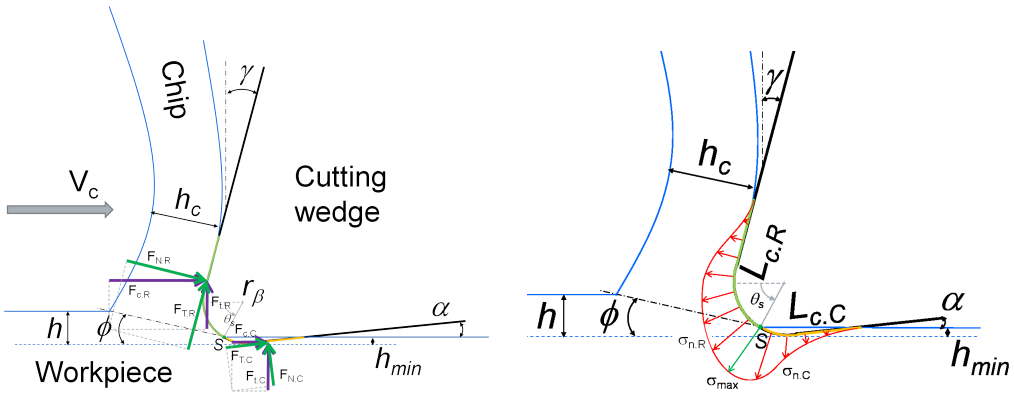

(a) Configuration and forces (b) Normal stress

Figure 1: Orthogonal cutting configuration.

These forces can be computed, assuming the chip equilibrium, from the following relation,

$$F_{shear} = \frac{\overline{\tau_s}\, b\, h}{\sin\phi}, \qquad F_{comp} = \frac{\overline{\tau_s}\, b\, h}{\sin\phi}\tan\left(\phi - \gamma + \lambda_R\right), \tag{2}$$

where $\overline{\tau_s}$ is the equivalent shear stress, h is the uncut chip thickness, b is the width of cut, $\lambda_R = \arctan\mu_R$ is the friction angle and γ is the rake angle. The formulation given by (Merchant 44), frequently used in numerical simulations, assume the shear band as infinitely thin. Assuming a perfect plastic material and a Coulomb's friction law, the shear angle is obtained by the minimisation of the cutting energy. The model proposed by (Lee 51) is also frequently used but some discrepancy where found using theses two models that are special cases of the Zworykin law (Zvorykin 93) given in the following equation.

$$\phi = C_{Z1} + C_{Z2}\left(\gamma - \lambda_R\right) \tag{3}$$

Due to strain rate $\dot{\varepsilon} > 10^3$ and true strain $\varepsilon \approx 1$, classical mechanics are not sufficient. (Thomsen 65) assumed a constant shear stress equal to the shear strength along the shear plane. (Shaw 80) assumed a normal and frictional stress distribution analogous to the one of Zorev. The model proposed by Johnson and Cook is the most used in numerical simulation (Pujana 07). This model is a thermo-viscoplastic law considering strain hardening and its application range is closed to those encountered in machining. Because of the lack of data on temperature, the model used to predict the equivalent stress state in the shear band is expressed by the following relation,

$$\overline{\tau_s} = \begin{cases} \frac{1}{\sqrt{3}}\,\sigma_1\,\overline{\varepsilon}^{\,m} & \text{if} \quad \overline{\varepsilon} \le 1 \\ \frac{1}{\sqrt{3}}\left[(1-m)\,\sigma_1 + m\,\sigma_1\,\overline{\varepsilon}\right] & \text{if} \quad \overline{\varepsilon} > 1 \end{cases}, \tag{4}$$

where σ_1 is the stress for a deformation $\overline{\varepsilon} = 1$ and m the stress hardening index. The deformation $\overline{\varepsilon}$ is usually estimated in the middle of the shear band as

$$\overline{\varepsilon} = \frac{1}{2}\,\frac{\cos\gamma_{eff}}{\sqrt{3}\sin\phi\,\cos\left(\phi - \gamma_{eff}\right)}, \tag{5}$$

from the visualisation method. Equation (5) is involving the effective rake angle γ_{eff}. This angle is usually considered in micro-machining (Outeiro 05) where the uncut chip thickness is inferior or close to the edge radius r_β as shown on figure 1.

The root of the shear band is assumed to be localised at the stagnation point S and the

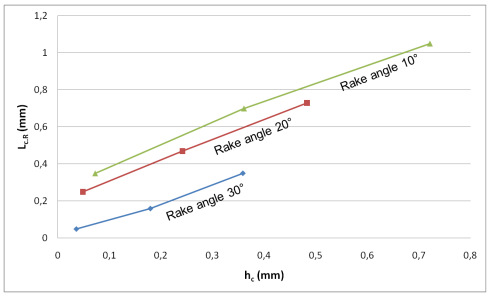

Figure 2: Relation between chip thickness h_c and contact length $L_{c,R}$.

stress is maximum. Then, the stress decreases along the rake face contact length to reach zero when the tool and the chip are no longer in contact as shown on figure 1b. The same type of distribution is assumed on the clearance face with a continuity with the rake face. Some results in the literature are suggesting the normal stress distribution on the rake face given in equation (6), where $L_{c,R}$ is the tool/chip contact length and $x \in [0, L_{c,R}]$.

$$\sigma_{n,R}(x) = \sigma_{max,R} \left(1 - \frac{x}{L_{c,R}}\right)^{n_R} \tag{6}$$

The experimental results available in the literature reveal that the exponent n_R, conditioning the curvature of the distribution, cannot be inferior to 1 and the the stress $\sigma_{max,R}$ is not always restricted to the tip of the tool (Barrow 82; Arsecularatne 97). Integrating equation (6) leads to

$$n_R = \frac{\sigma_{max,R}\, b\, L_{c,R}}{F_{N,R}} - 1, \tag{7}$$

where $F_{N,R}$ is the normal force acting on the rake face due to the action of the chip. The tool/chip contact length $L_{c,R}$ is dependant of the chip thickness h_c (8). As shown on figure 2, the more the chip is thick, the less it can bend, which increases its contact length on the rake face.

$$h_c = \frac{h \cos(\phi - \gamma)}{\sin \phi} \tag{8}$$

The length $L_{c,R}$ is then obtained for a positive rake angle by the folowing equation

$$L_{c,R} = h_c - \zeta_1 \gamma + \zeta_2, \tag{9}$$

where ζ_1 and ζ_2 are empirical constants. The stress $\sigma_{max,R}$ is obtained from the Hencky's theorem $p + 2\tau\psi = constant$ (Oxley 77). The normal stress at the stagnation point S is then computed from

$$\sigma_{max,R} = 2\tau_s \tan(\phi + \lambda_R - \gamma) - \tau_s \left[1 + 2\left(\frac{\pi}{4} - \phi\right)\right] + \tau_s \sin 2(\gamma - \phi). \tag{10}$$

Assuming a constant friction coefficient μ, the frictional stress is expressed from

$$\tau_{f,R}(x) = \begin{cases} \tau_p & \text{if} \quad \mu\, \sigma_{n,R} \geq \tau_p \\ \mu\, \sigma_{n,R}(x) & \text{if} \quad \mu\, \sigma_{n,R} < \tau_p \end{cases}, \tag{11}$$

were $\tau_p = \frac{\sigma_y}{\sqrt{3}}$ and σ_y the yield stress.

2.2 Forces on the clearance face

The forces acting on the clearance face are usually neglected in force modelling because of the importance of the forces generated in the primary shear zone. In superfinish machining, as in micro-machining, the separation of the work material is affected by the sharpness of the edge. The two main approaches considers a stagnation point, as (Albrecht 60), or a dead metal zone acting as a stable built-up edge indenting the work material (Abdelmoneim 74). In this work, the forces generated on each face of the tool are independent and the work material is divided around a stagnation point. To compute the stresses on the clearance face, a continuity with the stresses on the rake face is assumed. The normal stress at the tool tip is still given by equation (10). The contact length between the clearance face of the tool and the machined surface is estimated from the dimension of the ploughed layer h_{min} and computed from equation (12). The parameter h_{min} is computed from the position of the stagnation point S. Its localisation is obtained from visualisation of the machined area and is given by the angle $\theta_s = \frac{5\pi}{36} - \gamma$ as visible on figure 1.

$$L_{c,C} = \left(\frac{\pi}{2} + \alpha - \theta_S\right) r_\beta + \frac{h_{min}}{\sin\alpha} \qquad \text{with} \qquad h_{min} = r_\beta\,(1 - \sin\theta_S), \tag{12}$$

where α is the clearance angle. Then, the same type of distribution as equation (6) is applied along $L_{c,C}$ as described on figure 1b. Finally, equations (6) and (11) are used with parameters related to the clearance face.

3 EXPERIMENTAL PROCEDURE

To calibrate the model, experimental data are required. Machining tests were performed on a SOMAB T400TD CNC lathe. ISO K20 Tungsten carbide tools were used. The input parameters are the rake angle γ, the clearance angle α, the feed rate f, the cutting speed V_c and the edge radius r_β that varies slightly on each tool in a range from 8 to 12 micrometres. The edge radii are measured using a stereoscopic method from SEM pictures. Orthogonal cutting tests were conducted on copper discs and tubes at constant cutting speed and feed rate. The parameters are listed in table I. This test configuration simplifies the cutting process as a two dimensional problem. The sample thickness is set to be approximately ten times the feed rate to achieve the plane state of both strain and stress hypothesis in the main shear zone (Grzesik 08).

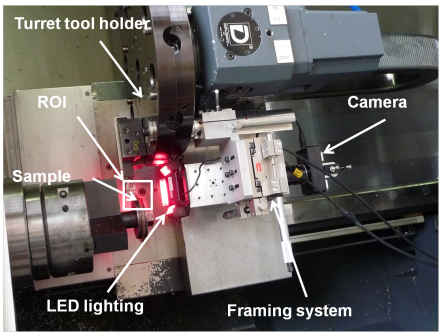

Figure 3: Experimental device.

Parameters	Unit	Levels
V_c	m/min	140
h	mm	0.01, 0.05, 0.1, 0.15, 0.2
γ	°	5, 10, 20, 30
α	°	5, 10, 20
r_β	µm	8 – 12

Table I: Test parameters.

In addition, a high resolution CMOS camera (figure 3) records images of the chip formation area in order to measure geometrical parameters such as the contact area between the tool and the machined surface. For all tests, forces, axial position, feed rate and spindle speed were

measured. Chip thickness is also measured to compute the shear angle ϕ according to the geometrical relation $\tan\phi = (h\cos\gamma)/(h_c - h\sin\gamma)$. A micro quantity lubrication device was used.

4 IDENTIFICATION OF THE MODEL

To use this model, some parameters have to be identified. For a large ratio $\frac{h}{r_\beta}$, the effects of the clearance face and edge radius are minimum and can be neglected. Then, in equation (1), it is allowed to assume $F_{c,C} = 0$ and $F_{t,C} = 0$. The constants C_{Z1} and C_{Z2} are obtained from curve fitting of equation (3) on experimentally observed shear angles ϕ. In the case of a large ratio $\frac{h}{r_\beta}$, the stress $\overline{\tau_s}$ can be expressed from $F_{c,R}$ and $F_{c,C}$. The figure 4 illustrates this hypothesis showing a rise of the apparent shear stress below a ratio of 5. The parameters σ_1 and m can be obtained from equation (4) by curve fitting along $\overline{\varepsilon}$. In the case of a computed exponent $n_R < 1$ this one is set to 1 and a plateau at $\sigma_{max,R}$ is generated until the force $F_{N,R}$ is reached. The corresponding exponent n_C on the clearance face is set to 1.

5 RESULTS AND DISCUSSION

As expected, the forces increase significantly with the reduction of the rake angle and slightly with the clearance angle. Small uncut chip thickness h against edge radius r_β has shown an important scale effect on force measurements for configurations with the ratio $\frac{h}{r_\beta} \leq 5$. The observations made by the camera helped to evaluate the contact with the workpiece. Despite the initial blur and the averaging effect of the post treatment, the images revealed a larger clearance contact area with tools of low rake angles. The model does not fit perfectly the experimental data as visible on figure 5. For the cutting force on figure 5a, the model cannot reach the experimental force level at the lowest depth of cut. The force prediction for a rake angle of 20° is also underestimated. The modelling of the thrust force on figure 5b presents also a lack of accuracy for the lowest depth of cut but fits relatively well the other configurations. To explain such divergence, several remarks have to be made. First of all, the force measurements are not perfectly reliable. For example, the force signals measured for the tools with a rake angle of 20° do not follow the same trend than for the other tools. Secondly, the friction on both rake and clearance faces is assumed as constant along the contact lengths $L_{c,R}$ and $L_{c,C}$. The variation of pressure between the separation point and the end of the contact length probably affects its value. Thirdly, the visualisation of the interference volume between the workpiece and the tool cannot ensure the modelling of the angle θ_S that rules the variable h_{min}, especially for the lowest depth of cut that are too blurred. At last, it can be argued that the force components acting on

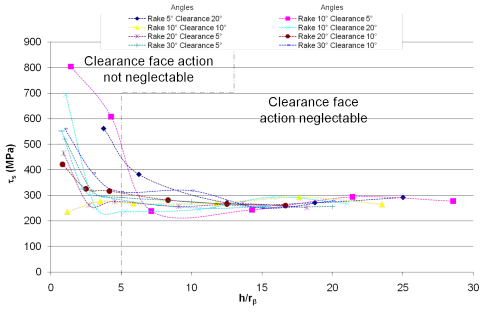

Figure 4: Apparent shear stress.

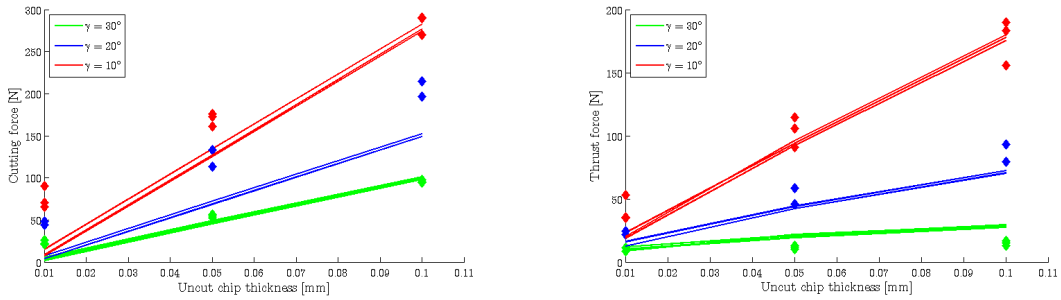

(a) Cutting force F_c (b) Thrust force F_t

Figure 5: Modelled (lines) and experimental (dots) forces.

the clearance face are not completely reliable. In addition, the distributions of the normal and tangential stresses are identified for a straight surface and then computed on a curved area. As maximum stress computed on the rake face remains steady along a certain range, a similar behaviour might exist on the clearance face.

6 CONCLUSIONS

The purpose of this study is to describe a model for the prediction of cutting forces at the scale of superfinishing operations on pure copper. This work material is very ductile which increases the phenomenon of ploughing. The model considers the forces acting on both rake and clearance faces. The forces computed on the rake face provide interesting results but the ploughing forces need to be improved. The observation with a camera is a helping device but is a little weak to observe the interaction of the tool with the machined surface. Developments have to be done on the estimation of the forces acting on the clearance face.

References:

[Abdelmoneim 74] M. E. Abdelmoneim & E. F. Scrutton. *TOOL EDGE ROUNDNESS AND STABLE BUILD-UP FORMATION IN FINISH MACHINING.* J Eng Ind Trans ASME, vol. 96 Ser B, no. 4, pages 1258–1267, 1974. Cited By (since 1996): 23.

[Albrecht 60] P. Albrecht. *New developments in the theory of metal cutting process: Part I - The ploughing process in metal cutting*. ASME J. Eng. Ind., vol. 82, pages 348–358, 1960. Cited By (since 1996): 65.

[Arsecularatne 97] J. A. Arsecularatne. *On tool-chip interface stress distributions, ploughing force and size effect in machining*. International Journal of Machine Tools and Manufacture, vol. 37, no. 7, pages 885–899, 7 1997.

[Barrow 82] G. Barrow, W. Graham, T. Kurimoto & Y. F. Leong. *Determination of rake face stress distribution in orthogonal machining*. International Journal of Machine Tool Design and Research, vol. 22, no. 1, pages 75–85, 1982.

[Grzesik 08] W. Grzesik. Orthogonal and oblique cutting mechanics, pages 69–84. Advanced Machining Processes of Metallic Materials. Elsevier, Amsterdam, 2008.

[Kienzle 52] O. Kienzle & H. Victor. *Die Bestimmung von Kra?ften und Leistungen an spanenden Werkzeugmaschinen*. VDI-Z, vol. 94, no. 11-12, pages 299–305, 1952. Cited By (since 1996): 16.

[Lee 51] E. H. Lee & B. W. Shaffer. *The theory of plasticity applied to the problem of machining*. Journal of Applied Mechanics, vol. 18, pages 405–413, 1951.

[Merchant 44] M. E. Merchant. *Basic mechanics of the metal cutting process*. Journal of Applied Mechanics, vol. 11, pages A168–A175, 1944.

[Outeiro 05] J. C. Outeiro & V. P. Astakhov. *The role of the relative tool sharpness in modelling of the cutting process*. Proc. 8th CIRP International Workshop on Modeling of Machining Operations, pages 517–523, 2005. Cited By (since 1996): 1.

[Oxley 77] P. L. B. Oxley & W. F. Hastings. *Predicting the Strain Rate in the Zone of Intense Shear in which the Chip is Formed in Machining from the Dynamic Flow Stress Properties of the Work Material and the Cutting Conditions*. Proceedings of the Royal Society of London.A.Mathematical and Physical Sciences, vol. 356, no. 1686, pages 395–410, September 15 1977.

[Pujana 07] J. Pujana, P. J. Arrazola, R. MSaoubi & H. Chandrasekaran. *Analysis of the inverse identification of constitutive equations applied in orthogonal cutting process*. International Journal of Machine Tools and Manufacture, vol. 47, no. 14, pages 2153–2161, 11 2007.

[Shaw 80] M. C. Shaw. *A new mechanism of plastic flow*. International Journal of Mechanical Sciences, vol. 22, no. 11, pages 673–686, 1980.

[Thomsen 65] E. G. Thomsen, C. T. Yang & S. Kobayashi. Mechanics of plastic deformation in metal processing. Macmillan, Collier-Macmillan (New York, Toronto), 1965.

[Zvorykin 93] K. A. Zvorykin. Proceedings of the Kharkov Technological Institute, 1893.

*** E-mail address: dimitri.germain@ensam.eu**
Tel.: +33 380 23 49 06/+33 385 59 53 88; fax: +33 380 23 52 21/+33 385 59 53 70.